

## Oxidation of a Water-Soluble Phosphine and Some Spectroscopic Probes with Nitric Oxide and Nitrous Acid in Aqueous Solutions<sup>†</sup>

Andreja Bakac,\* Margaret Schouten, Alicia Johnson, Wenjing Song, Oleg Pestovsky, and Ewa Szajna-Fuller

Iowa State University, Ames, Iowa 50011

Received April 8, 2009

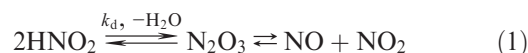
In acidic aqueous solutions, nitrogen monoxide oxidizes monosulfonated triphenylphosphine, TPPMS<sup>−</sup>, to the corresponding phosphine oxide. The NO-derived product is N<sub>2</sub>O. This chemistry parallels that reported for the reaction of NO with the unsubstituted triphenylphosphine in nonpolar organic solvents, but the rate constant measured in this work,  $5.14 \times 10^6 \text{ M}^{-2} \text{ s}^{-1}$ , is greater by several orders of magnitude. This makes TPPMS<sup>−</sup> a useful analytical reagent for NO in aqueous solution. The increased rate constant in the present work appears to be a medium effect, and unrelated to the introduction of a single sulfonate group in the phosphine. The reaction between nitrous acid and TPPMS<sup>−</sup> has a 2:1 [TPPMS<sup>−</sup>]/[HNO<sub>2</sub>] stoichiometry and generates NH<sub>2</sub>OH quantitatively. The rate law,  $\text{rate} = 4k_d[\text{HNO}_2]^2[\text{TPPMS}^-]$ , identifies the second-order self-reaction of HNO<sub>2</sub> as the rate-limiting step that generates the active oxidant(s) for the fast subsequent reaction with TPPMS<sup>−</sup>. It appears that the active oxidant is N<sub>2</sub>O<sub>3</sub>, although the oxides NO and NO<sub>2</sub> derived from it may be also involved. Bimolecular self-reaction of HNO<sub>2</sub> also precedes the oxidations of ABTS<sup>2−</sup> and TMPD. Competing with this path are the acid-catalyzed oxidations of both reagents via NO<sup>+</sup>.

### Introduction

Nitrite and nitrogen oxides play important roles in various biological processes in mammals<sup>1</sup> and plants,<sup>2,3</sup> in nitrogen dynamics in soil,<sup>4</sup> atmospheric (photo)chemistry,<sup>5</sup> and in the laboratory. The first example of nitrite acting as electron donor for anoxygenic photosynthesis has also been discovered recently.<sup>6</sup>

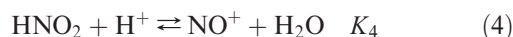
In view of their widespread involvement in nature, nitrogen oxides and nitrite/nitrous acid have been a subject of numerous mechanistic studies.<sup>7–11</sup> One of the mechanisms by which nitrous acid reacts with substrates involves the disproportionation of HNO<sub>2</sub> followed by the reaction of one or both nitrogen oxides with the substrate, as shown in eq 1 and 2.<sup>12,13</sup>

For a number of reactive substrates the step(s) in eq 2 is fast relative to both forward and reverse steps in eq 1. Under those circumstances, the kinetics become second order in [HNO<sub>2</sub>] and zero-order in [substrate], eq 3, where  $k_d = (10.9 + 175 [\text{H}^+]) \text{ M}^{-1} \text{ s}^{-1}$  in acidic aqueous solutions at 25 °C,<sup>13</sup> and  $n$  is the stoichiometric factor, i.e., the number of equivalents of substrate consumed per rate-determining step.



$$-d[\text{substrate}]/dt = nk_d[\text{HNO}_2]^2 \quad (3)$$

Another common mechanism for oxidations with nitrous acid involves acid-catalyzed formation of NO<sup>+</sup> (or H<sub>2</sub>NO<sub>2</sub><sup>+</sup>) followed by the oxidation of substrates with NO<sup>+</sup>, eqs 4 and 5. The rate law, eq 6, is first-order in each [H<sup>+</sup>], [HNO<sub>2</sub>], and [substrate], which makes this mechanism kinetically distinguishable from the disproportionation mechanism above.



$$-d[\text{substrate}]/dt = k_5K_4[\text{HNO}_2][\text{H}^+][\text{substrate}] \quad (6)$$

Nitrogen dioxide, generated in eq 1, might be expected to act as an oxygen atom donor toward convenient acceptors,

<sup>†</sup> Reported in part at the 235th ACS National Meeting in New Orleans

\*To whom correspondence should be addressed. E-mail: bakac@ameslab.

gov.  
(1) *Nitric Oxide. Biology and Pathobiology*; Ignarro, L. J., Ed.; Academic: San Diego, 2000.

(2) Neill, S. J.; Desikan, R.; Hancock, J. T. *New Phytol.* **2003**, *159*, 11–35.

(3) Crawford, N. M. *J. Exp. Bot.* **2006**, *57*, 471–478.

(4) Van Cleemput, O.; Samater, A. H. *Fert. Res.* **1996**, *45*, 81–89.

(5) Vione, D.; Maurino, V.; Minero, C.; Pelizzetti, E.; Harrison, M. A. J.; Olariu, R.-I.; Arsene, C. *Chem. Soc. Rev.* **2006**, *35*, 441–453.

(6) Griffin, B. M.; Schott, J.; Schink, B. *Science* **2007**, *316*, 1870.

(7) Ford, P. C.; Laverman, L. E. *Coord. Chem. Rev.* **2005**, *249*, 391–403.

(8) Goldstein, S.; Czapski, G. *Inorg. Chem.* **1995**, *34*, 4041–4048.

(9) Roncaroli, F.; Videla, M.; Slep, L. D.; Olabe, J. A. *Coord. Chem. Rev.*

**2007**, *251*, 1903–1930.

(10) Wolak, M.; van Eldik, R. *Coord. Chem. Rev.* **2002**, *230*, 263–282.

(11) Bakac, A. *Adv. Inorg. Chem.* **2004**, *55*, 1–59.

(12) Stedman, G. *Adv. Inorg. Chem. Radiochem.* **1979**, *22*, 113–170.

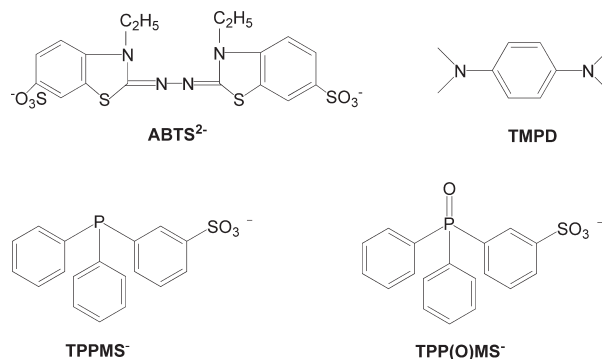
(13) Pestovsky, O.; Bakac, A. *Inorg. Chem.* **2002**, *41*, 901–905.

but the available data do not support that notion. Even though a number of cases of photochemically induced oxygen atom transfer (OAT) from  $\text{NO}_2$  have been published,<sup>14–16</sup> the data on thermal OAT to typical oxygen acceptors are quite limited. Even when net OAT does occur, as in the oxidation of thioethers<sup>17</sup> or olefins,<sup>18</sup> the reaction requires initiation by electron transfer. In the former reaction, the nitrosonium donor–acceptor complex  $[\text{R}_2\text{S}, \text{NO}^+] \text{NO}_3^-$  is a critical intermediate generated by thioether-induced disproportionation of  $\text{NO}_2$ .<sup>17</sup> The oxidation of olefins<sup>18</sup> requires electron transfer to generate olefin cation radicals, followed by OAT from  $\text{NO}_2$ . We are not aware of any kinetic data even for reactions with “standard” oxygen atom acceptors, such as  $\text{PPh}_3$ .

The  $\text{NO}_2/\text{PPh}_3$  reaction to generate  $\text{NO}$  and  $\text{OPPh}_3$  is thermodynamically favorable. For a gas-phase reaction, a standard enthalpy change  $\Delta H_r^0$  is about  $-50$  kcal/mol, as calculated from the standard thermochemical data and assuming that the enthalpies of sublimation of  $\text{PPh}_3$  and  $\text{PPh}_3\text{O}$  are not greatly different. Oxidation of  $\text{PPh}_3$  to the corresponding oxide is among the most common and convenient reactions that allow one to gauge the ability of an oxidant to act as an oxygen atom donor. One-electron oxidation of  $\text{PPh}_3$ , which will ultimately also yield the oxide  $\text{OPPh}_3$ , is limited to strong 1-e oxidants because of the rather high reduction potential for the  $\text{PPh}_3^{\bullet+}/\text{PPh}_3$  couple.<sup>19–21</sup>

The reaction of nitrogen monoxide with  $\text{PPh}_3$ , on the other hand, has been studied, although not in aqueous solutions.<sup>22,23</sup> The products,  $\text{N}_2\text{O}$  and  $\text{OPPh}_3$ , were generated in a kinetically third-order process,  $\text{rate} = k[\text{PPh}_3][\text{NO}]^2$ , that exhibited strong dependence on solvent polarity and phosphine basicity in a series of para-substituted triarylphosphines.

The complete lack of data on the reactivity of  $\text{NO}_2$  toward oxygen atom acceptors, and the availability of  $\text{NO}/\text{PPh}_3$  data only in nonaqueous solutions prompted us to examine the reaction of nitrous acid as a convenient source of both  $\text{NO}$  and  $\text{NO}_2$  with a phosphine. Because the biological chemistry of nitrite and nitrogen oxides typically takes place in an aqueous milieu, the phosphine that we selected for this study is the water-soluble  $\text{P}(\text{C}_6\text{H}_5)_2(3\text{-SO}_3-\text{C}_6\text{H}_4)^-$  (hereafter  $\text{TPPMS}^-$ ). The reactions of nitrous acid with two one-electron donors, tetramethylphenylene diamine (TMPD) and 2,2'-azino-bis(3-ethylbenzothiazoline-6-sulfonate ( $\text{ABTS}^{2-}$ )), were also examined. The structures of various reagents used in this work are shown below.



## Experimental Section

2,2'-Azino-bis(3-ethylbenzothiazoline-6-sulfonic acid) diammonium salt ( $(\text{NH}_4)_2\text{ABTS}$ , 98% pure), *N,N,N',N'*-tetramethyl-*para*-phenylenediamine (TMPD, 99% pure), and ninhydrin were purchased from Sigma Aldrich. Diphenylphosphinobenzene-3-sulfonic acid sodium salt,  $\text{Na}[\text{P}(\text{C}_6\text{H}_5)_2(\text{meta-SO}_3-\text{C}_6\text{H}_4)]$  ( $\text{NaTPPMS}$ , >90% pure), was obtained from TCI America and used as received. In-house distilled water was further purified by passage through a Barnstead EASY-pure III setup. The ionic strength was maintained at 0.10 or 1.0 M with  $\text{HClO}_4$  and  $\text{LiClO}_4$ .

Solutions of nitrous acid were generated in situ by addition of the appropriate amount of 0.10 M  $\text{HClO}_4$  into a spectrophotometric cell containing sodium nitrite (99.999%, Fisher). Gaseous  $\text{NO}$  (Matheson) was purified by passage through Ascarite, sodium hydroxide and water.<sup>24</sup> Stock solutions of  $\text{NO}$  were prepared by bubbling the purified gas through argon-saturated solutions of desired acidity ( $\text{HClO}_4$ ) for 30 min. Such a solution typically contained 1.7 mM  $\text{NO}$  and 0.2–0.3 mM total nitrite.<sup>25</sup> Hydroxylamine was detected and quantified with ninhydrin, which reacts with primary amines to yield the intensely blue product,  $\lambda_{\text{max}}$  580 nm.<sup>26–28</sup> The molar absorptivity of the product, determined in calibration experiments with known amounts of hydroxylamine, was found to be  $4910 \text{ M}^{-1} \text{ cm}^{-1}$ . The results were confirmed with another test that involved the reduction of  $\text{Fe}(\text{phen})_3^{3+}$ . The reaction solution was mixed with aqueous  $\text{Fe}(\text{III})$  and phenanthroline (1:3 ratio) in aqueous acetate buffer (pH 4.2), and the absorbance increase was monitored at the 510 nm maximum of  $\text{Fe}(\text{phen})_3^{2+}$  ( $\epsilon = 1.14 \times 10^4 \text{ M}^{-1} \text{ cm}^{-1}$ ). The rate constant matched that measured independently with genuine  $\text{NH}_2\text{OH}$  under the same conditions. The concentration of  $\text{NH}_2\text{OH}$  was calculated from the absorbance increase using the independently established 1:1  $[\text{Fe}(\text{III})]:[\text{NH}_2\text{OH}]$  stoichiometry.

Kinetic measurements were initiated by injecting the desired substrate ( $\text{ABTS}^{2-}$ , TMPD, or  $\text{TPPMS}^-$ ) into a spectrophotometric cell containing all the other reagents. The absorbance change was monitored by conventional spectrophotometry (Shimadzu 3101 PC) at a wavelength of maximum absorbance of  $\text{ABTS}^{\bullet-}$ ,  $\text{TMPD}^{\bullet+}$ , or  $\text{TPPMS}^-$ . The kinetics of the  $\text{NO}/\text{TPPMS}^-$  reaction were too fast for this method and required a stopped flow (Applied Photophysics DX 17 MV). Ionic strength was adjusted with  $\text{HClO}_4$  and  $\text{LiClO}_4$ . All of the kinetic data were obtained at  $25.0 \pm 0.2$  °C under air-free conditions (argon atmosphere). Kinetic analyses were performed with KaleidaGraph 3.6 PC software.

The solid  $\text{NaTPPMS}$  used in this work was found to contain ~9% (by molar ratio) unreactive impurities, most

(14) Tanaka, N.; Oike, J.; Shibuya, K.; Kudoh, S.; Nakata, M. *Res. Chem. Int.* **1998**, *24*, 893–903.

(15) Harrison, J. A.; Frei, H. *J. Phys. Chem.* **1994**, *98*, 12152–12157.

(16) Nakata, M. *Spectrochim. Acta, Part A* **1994**, *50A*, 1455–1465.

(17) Bosch, E.; Kochi, J. K. *J. Org. Chem.* **1995**, *60*, 3172–3183.

(18) Bosch, E.; Kochi, J. K. *J. Am. Chem. Soc.* **1996**, *118*, 1319–1329.

(19) Yasui, S.; Kenji, I.; Ohno, A. *Heteroatom Chem.* **2001**, *12*, 217–222.

(20) Nakamura, M.; Miki, M.; Majima, T. *J. Chem. Soc., Perkin Trans. 2* **2000**, 1447–1452.

(21) Shinro, Y.; Tsujimoto, M.; Kosei, S.; A., O. *Chem. Ber./Recueil* **1997**, *130*, 1699–1707.

(22) Lim, M. D.; Lorkovic, I. M.; Ford, P. C. *Inorg. Chem.* **2002**, *41*, 1026–1028.

(23) Longhi, R.; Ragsdale, R. O.; Drago, R. S. *Inorg. Chem.* **1962**, *1*, 768–770.

(24) Pestovsky, O.; Bakac, A. *J. Am. Chem. Soc.* **2002**, *124*, 1698–1703.

(25) Song, W.; Bakac, A. *Chem.—Eur. J.* **2008**, *14*, 4906–4912.

(26) Moore, S.; Stein, W. *J. Biol. Chem.* **1948**, *176*, 367.

(27) Moore, S.; Stein, W. *J. Biol. Chem.* **1954**, *211*, 907.

(28) Moore, S. *J. Biol. Chem.* **1968**, *243*, 6281.

**Table 1.** Spectral Data for Some Species in this Work<sup>a</sup>

species	$\epsilon (\times 10^3 \text{ M}^{-1} \text{ cm}^{-1}) ([\text{H}^+]/\text{M})$		
	$\lambda = 259 \text{ nm}$	$\lambda = 266 \text{ nm}$	$\lambda = 369 \text{ nm}$
TPPMS <sup>-</sup>	9.69 (0.10)		
	11.2 (0.005)		
TPP(O)MS <sup>-</sup>	1.59 (0.10)	2.08 (0.10)	
	1.70 (0.005)		
HNO <sub>2</sub>			0.050 (0.10)

<sup>a</sup>Mixture of TPPMS<sup>-</sup> and TPP(H)MS.

likely moisture and water of crystallization. Such solutions were only moderately stable toward autoxidation (~5% degradation in 24 h by UV-vis). Most experiments were carried out with freshly prepared solutions and/or under anaerobic conditions.

Molar absorptivities of TPPMS<sup>-</sup> ( $\lambda_{\text{max}}$  259 nm) and its oxidized form, TPP(O)MS<sup>-</sup>, were obtained by oxidizing TPPMS<sup>-</sup> (~160  $\mu\text{M}$ ) with a limiting amount of hydrogen peroxide (33.5  $\mu\text{M}$ , standardized with TiOSO<sub>4</sub>)<sup>29</sup> under anaerobic conditions in 0.10 M HClO<sub>4</sub>. This experiment provided the values of  $\Delta\epsilon_{259} = 8.10 \times 10^3 \text{ M}^{-1} \text{ cm}^{-1}$  (0.10 M HClO<sub>4</sub>) and  $9.5 \times 10^3 \text{ M}^{-1} \text{ cm}^{-1}$  (5.0 mM HClO<sub>4</sub>). Another sample of TPPMS<sup>-</sup> was oxidized with a slight excess of H<sub>2</sub>O<sub>2</sub>. The absorbance change at 259 nm was used to calculate the absolute concentration of TPPMS<sup>-</sup> in the sample, which led to the molar absorptivities in Table 1. All of the TPPMS<sup>-</sup> solutions in this work were standardized by UV-vis spectrophotometry at 259 nm.

The acidity constant  $K_{\text{aP}}$  of TPP(H)MS was determined from the effect of  $[\text{H}^+]$  (0.01–0.10 M HClO<sub>4</sub>) on the absorbance of the phosphine (100  $\mu\text{M}$ ) at 259 nm under anaerobic conditions and 0.10 M ionic strength (HClO<sub>4</sub> + NaClO<sub>4</sub>). The data were fitted to eq 7, where  $\text{Abs}_{\text{obs}}$  represents the measured absorbance in the presence of added  $\text{H}^+$ ,  $\text{Abs}_{\text{P}}$  is the absorbance in the absence of added  $\text{H}^+$ , and  $\epsilon_{\text{HP}}$  and  $\epsilon_{\text{P}}$  are the molar absorptivities of TPP(H)MS and TPPMS<sup>-</sup>, respectively.

$$\frac{\text{Abs}_{\text{obs}}}{\text{Abs}_{\text{P}}} = \frac{1}{[\text{H}^+] + K_{\text{aP}}} \times (K_{\text{aP}} + \epsilon_{\text{HP}}/\epsilon_{\text{P}} \times [\text{H}^+]) \quad (7)$$

Figure 1 shows the fit of the experimental data to eq 7 which yielded  $K_{\text{aP}} = 0.49 \pm 0.05 \text{ M}$  and  $\epsilon_{\text{HP}}/\epsilon_{\text{P}} = 0.30 \pm 0.06$ . Similar, but much less precise data were obtained in an earlier study at variable ionic strength which resulted in  $\text{H}^+$ -dependent  $K_{\text{aP}}$ .<sup>30</sup>

## Results

**TMPD/HNO<sub>2</sub> Reaction.** Upon mixing of the two reagents under air-free conditions, the solution turned dark blue, indicative of the formation of the radical cation  $\text{TMPD}^{\bullet+}$ . The kinetics were monitored at 610 nm where the molar absorptivity of the radical cation is  $8600 \text{ M}^{-1} \text{ cm}^{-1}$ .<sup>31</sup> The reaction stoichiometry, expressed as  $\Delta[\text{TMPD}^{\bullet+}]/\Delta[\text{HNO}_2]$ , was cleanly 1.0 when TMPD was used in large excess. When TMPD was limiting, the initial build-up of the blue radical cation was followed by its disappearance. We interpret these data to mean that the radical cation also reacted with HNO<sub>2</sub> to generate a much less absorbing species,  $\text{TMPD}^{2+}$ ,<sup>32</sup> in agreement with the known reaction between NO<sub>2</sub> and  $\text{TMPD}^{\bullet+}$ ,  $k = 1.3 \times 10^4 \text{ M}^{-1} \text{ s}^{-1}$  at pH 5.5, 40% CH<sub>3</sub>CN/H<sub>2</sub>O.<sup>33</sup>

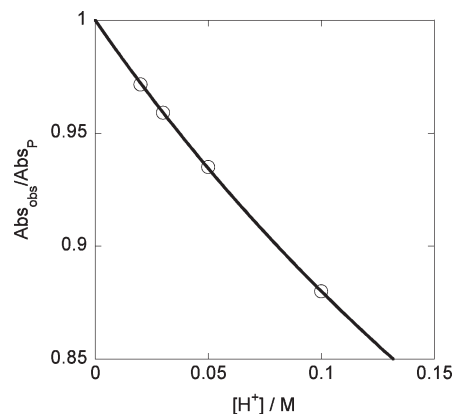


**Figure 1.** Plot of  $\text{Abs}_{\text{obs}}/\text{Abs}_{\text{P}}$  against  $[\text{H}^+]$  for the protonation of TPPMS<sup>-</sup>. Conditions:  $\lambda = 259 \text{ nm}$ , 100  $\mu\text{M}$  TPPMS<sup>-</sup>, 0.02–0.10 M HClO<sub>4</sub>, 0.10 M ionic strength, argon atmosphere. The solid line is a fit to eq 7.

To avoid interference from the secondary  $\text{TMPD}^{\bullet+}/\text{HNO}_2$  reaction, we studied the kinetics by the initial rate method. Concentrations were varied over a wide range and included runs with either one or the other reagent in excess. The ionic strength was kept at 1.0 M. In the acidity range used,  $5 \text{ mM} \geq [\text{H}^+] \geq 2 \text{ mM}$ , TMPD exists as a mixture of singly and doubly protonated forms ( $K_{\text{a1}} = 6.3 \times 10^{-3} \text{ M}$ ),<sup>34</sup> and nitrous acid as a mixture of HNO<sub>2</sub> and NO<sub>2</sub><sup>-</sup> ( $K_{\text{a}} = 6.3 \times 10^{-4} \text{ M}$ ).<sup>35</sup>

The initial rates were independent of the concentration of TMPD, and linearly dependent on  $[\text{HNO}_2]^2$ . By expressing the concentration of HNO<sub>2</sub> in terms of total concentration ( $[\text{HNO}_2]_{\text{tot}} = [\text{HNO}_2] + [\text{NO}_2^-]$ ), eq 8, one obtains the relation in eq 9, which suggests a plot described by eq 10, where  $R_i$  stands for initial rate.

$$[\text{HNO}_2] = \frac{[\text{H}^+]}{K_{\text{a}} + [\text{H}^+]} [\text{HNO}_2]_{\text{tot}} \quad (8)$$

$$R_i = k_{\text{obs}}[\text{HNO}_2]^2 = k_{\text{obs}} \left( \frac{[\text{H}^+]}{K_{\text{a}} + [\text{H}^+]} [\text{HNO}_2]_{\text{tot}} \right)^2 \quad (9)$$

$$\frac{R_i(K_{\text{a}} + [\text{H}^+])^2}{[\text{H}^+]^2} = k_{\text{obs}}[\text{HNO}_2]_{\text{tot}}^2 \quad (10)$$

The fit, shown in Figure 2 yielded  $k_{\text{obs}} = 12.3 \pm 0.3 \text{ M}^{-1} \text{ s}^{-1}$ . At the acid concentrations used, the values of  $k_{\text{d}}$  calculated for the mechanism in eqs 1–3 from the parameters established in our earlier work<sup>13</sup> range from  $11.2 \text{ M}^{-1} \text{ s}^{-1}$  (2 mM H<sup>+</sup>) to  $11.8 \text{ M}^{-1} \text{ s}^{-1}$  (5 mM H<sup>+</sup>). The experimental value derived above agrees with this calculation to within less than 10% and strongly supports the mechanism in eqs 1–3. Because NO does not react with TMPD, see below, the observed 1:1 [TMPD]/[HNO<sub>2</sub>] stoichiometry requires that each molecule of NO<sub>2</sub> oxidizes two molecules of TMPD.

**ABTS<sup>2-</sup>/HNO<sub>2</sub> Reaction.** Kinetic traces were exponential when  $[\text{ABTS}^{2-}]$  (0.2–0.8 mM) was present in large

(29) Pestovsky, O.; Bakac, A. *J. Am. Chem. Soc.* **2004**, *126*, 13757–13764.

(30) Wright, G.; Bjerum, J. *Acta Chem. Scand.* **1962**, *16*, 1262–1270.

(31) Rao, P. S.; Hayon, E. *J. Phys. Chem.* **1975**, *79*, 1063–1066.

(32) Chaka, G.; Bakac, A. *Dalton Trans.* **2009**, 318–321.

(33) Pestovsky, O.; Bakac, A. *Inorg. Chem.* **2003**, *42*, 1744–1750.

(34) Neta, P.; Huie, R. E. *J. Phys. Chem.* **1985**, *89*, 1783–1787.

(35) Greenwood, N. N.; Earnshaw, A. *Chemistry of the Elements*, 2nd ed.; Oxford University Press: New York, 1997.

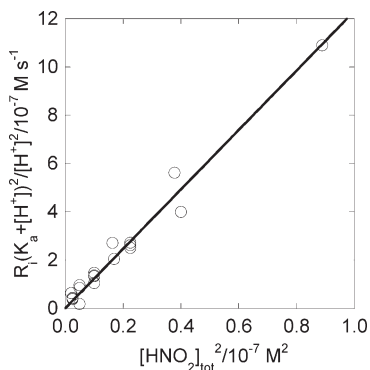


**Figure 2.** Plot of the initial rate of formation of  $\text{TMPD}^{+}$ , adjusted for the proportion of  $[\text{HNO}_2]$  present as nitrite, against the square of the total concentration of  $\text{HNO}_2$ . Conditions:  $[\text{TMPD}] = (1-30) \times 10^{-5} \text{ M}$ ,  $[\text{HNO}_2] = (5-30) \times 10^{-5} \text{ M}$ ,  $[\text{H}^+] = (2.0-5.0) \times 10^{-3} \text{ M}$ , ionic strength 1.0 M.

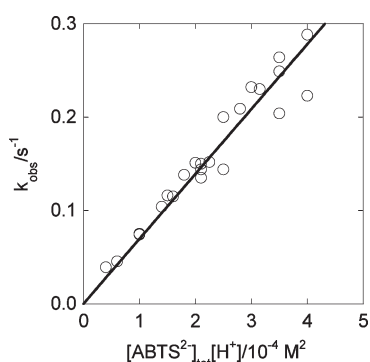


**Figure 3.** Plot of  $k_{\text{obs}}$  vs  $[\text{ABTS}^{2-}]_{\text{tot}}[\text{H}^+]$  for the reaction of  $\text{HNO}_2$  (0.01–0.1 mM) with excess  $\text{ABTS}^{2-}$  (0.2–0.8 mM) at 0.20–0.80 M  $\text{H}^+$  and 1.0 M ionic strength.

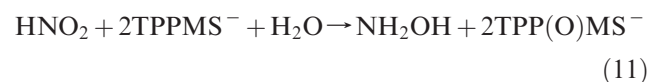
excess over  $[\text{HNO}_2]$  (0.01–0.10 mM), and yielded pseudo-first-order rate constants that exhibited first-order dependence on each  $[\text{ABTS}^{2-}]$  and  $[\text{H}^+]$ . A plot of  $k_{\text{obs}}$  against the product  $[\text{ABTS}^{2-}]_{\text{tot}} \times [\text{H}^+]$  at 1.0 M ionic strength, shown in Figure 3, yielded the value of the third-order rate constant,  $k_A = 695 \pm 16 \text{ M}^{-2} \text{ s}^{-1}$ . The concentration of  $\text{H}^+$  was varied in these experiments over the range 0.20–0.80 M. Under these conditions, most of  $\text{ABTS}^{2-}$  exists as a singly protonated species,  $\text{HABTS}^-$ ,  $pK_a = 2.08$ .<sup>36</sup> Surprisingly, when a correction was made for the protonated fraction, and the corrected value used in a plot analogous to that in Figure 3, i.e., assuming that only the dianion  $\text{ABTS}^{2-}$  was reactive, the data strongly deviated from linearity. Clearly,  $\text{ABTS}^{2-}$  is not much more reactive than  $\text{HABTS}^-$ .

The data are consistent with the mechanism shown in eqs 4–6, with both  $\text{ABTS}^{2-}$  and  $\text{HABTS}^-$  reacting with  $\text{NO}^+$ , and  $k_A = K_4 k_5$ . For  $K_4 = 3 \times 10^{-7} \text{ M}^{-1}$ ,<sup>37</sup> one obtains  $k_5 = (2.32 \pm 0.05) \times 10^9 \text{ M}^{-1} \text{ s}^{-1}$ . In view of the rate constant being close to diffusion-controlled value, it is not surprising that the reactivity is not greatly affected by converting  $\text{ABTS}^{2-}$  ( $E^0 = 0.68 \text{ V}$ ) to a somewhat less reducing  $\text{HABTS}^-$  ( $E^0 = 0.81 \text{ V}$ ).<sup>36</sup>

The kinetic behavior changed at higher concentrations of  $\text{HNO}_2$  when  $\text{ABTS}^{2-}$  became the limiting reagent. The appearance of the kinetic plots was close to second-order, especially at low  $[\text{H}^+]$  ( $< 0.05 \text{ M}$ ). Initial rates were used to calculate the second-order rate constants  $k_{\text{HNO}_2}$  under the assumption that the mechanism in eqs 1–3 dominates. Data analysis, analogous to that outlined above for  $\text{TMPD}$ , yielded the second-order rate constants of  $16.5 \text{ M}^{-1} \text{ s}^{-1}$  at 0.010 M  $\text{H}^+$  and  $19.8 \text{ M}^{-1} \text{ s}^{-1}$  at 0.05 M  $\text{H}^+$ , close to the expected values, 12.7 and  $19.6 \text{ M}^{-1} \text{ s}^{-1}$ , respectively. These calculations assumed an overall 1:1  $[\text{HNO}_2]/[\text{ABTS}^{2-}]$  stoichiometry based on the lack of reactivity of  $\text{ABTS}^{2-}$  toward  $\text{NO}$  and the 2:1  $[\text{ABTS}^{2-}]/[\text{NO}_2]$  stoichiometry.

**TPPMS<sup>-</sup>/HNO<sub>2</sub> Reaction.** The stoichiometry was determined with either reagent in excess. In experiments with excess  $\text{HNO}_2$ , the absorbance change corresponding to the oxidation of  $\text{TPPMS}^-$  to  $\text{TPP(O)MS}^-$  was measured at 259 nm ( $\Delta\epsilon_{259} = 8.10 \times 10^3 \text{ M}^{-1} \text{ cm}^{-1}$ ), 290 nm ( $\Delta\epsilon_{290} = 3.48 \times 10^3$ ) or 300 nm ( $\Delta\epsilon_{300} = 1.43 \times 10^3$ ). When excess  $\text{TPPMS}^-$  was employed, the stoichiometry was determined from the absorbance change at either 369 nm ( $\epsilon_{\text{HNO}_2} = 50 \text{ M}^{-1} \text{ cm}^{-1}$ ) or a convenient wavelength below 300 nm where  $\text{TPPMS}^-$  absorbs. Throughout the range of concentrations used, i.e.,  $1.0 \text{ mM} \geq [\text{HNO}_2] \geq 0.02 \text{ mM}$  and  $1.0 \text{ mM} \geq [\text{TPPMS}^-] \geq 0.1 \text{ mM}$ , and regardless of which reagent was in excess, the overall stoichiometry,  $[\text{TPP(O)MS}^-]_{\text{inf}}/\Delta[\text{HNO}_2]$ , was in the range  $1.9 \pm 0.1$ .

Consistent with this stoichiometry, the  $\text{HNO}_2$ -derived product was hydroxylamine. In an experiment starting with 1.0 mM  $\text{TPPMS}^-$  and 1.0 mM  $\text{HNO}_2$  in 5.0 mM  $\text{HClO}_4$ , all of the  $\text{TPPMS}^-$  was oxidized, and the final concentration of  $\text{NH}_2\text{OH}$  was  $0.51 \pm 0.03 \text{ mM}$  (average of two determinations) by ninhydrin method, and  $0.41 \pm 0.01$  by iron phenanthroline method. The reaction is thus described by eq 11.



The kinetic data were obtained by the method of initial rates at 2.0–5.0 mM  $\text{HClO}_4$ . The rate of the formation of  $\text{TPP(O)MS}^-$  was second order in  $[\text{HNO}_2]$  and independent of  $[\text{TPPMS}^-]$  as shown in Figure 4 which yielded  $k = 39.0 \pm 1.6 \text{ M}^{-1} \text{ s}^{-1}$ , close to the calculated value of  $4k_d$  (defined in eq 1) in this acidity range (i.e.,  $45 \text{ M}^{-1} \text{ s}^{-1}$  at 2 mM  $\text{H}^+$ , and  $47 \text{ M}^{-1} \text{ s}^{-1}$  at 5 mM  $\text{H}^+$ ). The rate law is given in eq 12.

$$\begin{aligned} -d[\text{TPPMS}^-]/dt &= -2d[\text{HNO}_2]/dt \\ &= 4k_d[\text{HNO}_2]^2 \end{aligned} \quad (12)$$

At higher acid concentrations, the appearance of the traces was still second-order, but the rate constants increased more than expected for the mechanism in eqs 1–3. As in the  $\text{ABTS}^{2-}$  reaction, it appears that the mechanism in eqs 4–6 begins to contribute as  $[\text{H}^+]$  increases. These conditions were not explored further.

**TPPMS<sup>-</sup>/NO Reaction.** The 2:1 stoichiometry was determined from the absorbance changes at 259 nm caused by the addition of limiting amounts of  $\text{NO}$  to an

(36) Scott, S. L.; Chen, W.-J.; Bakac, A.; Espenson, J. H. *J. Phys. Chem.* **1993**, *97*, 6710–6714.

(37) Bayliss, N. S.; Dingle, R.; Watts, D. W.; Wilkie, R. *J. Aust. J. Chem.* **1963**, *16*, 933–942.

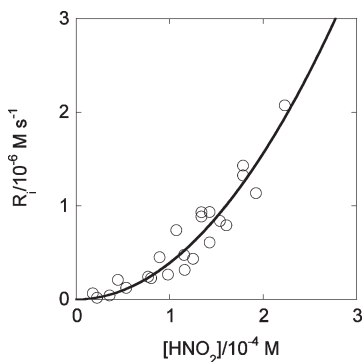


**Figure 4.** Dependence of initial rate for the TPPMS<sup>-</sup>/HNO<sub>2</sub> reaction on [HNO<sub>2</sub>]. Conditions: [TPPMS<sup>-</sup>] = (2–30) × 10<sup>-5</sup> M, [HNO<sub>2</sub>] = (2–25) × 10<sup>-5</sup> M, [H<sup>+</sup>] = 2–5 mM, ionic strength 0.10 M. The line is a fit to second-order kinetics with  $k = 39.0 \pm 1.6 \text{ M}^{-1} \text{ s}^{-1}$ .

excess of TPPMS<sup>-</sup>. The formation of N<sub>2</sub>O as reaction product was confirmed by GC-MS. The overall reaction is shown in eq 13.



The kinetics were studied under pseudo-first-order conditions using a large excess of NO over TPPMS<sup>-</sup>. A plot of the observed pseudo-first-order rate constants against [NO]<sup>2</sup> is linear, Figure 5, confirming the second-order dependence on [NO], eq 14, and yielding  $k_{13} = (5.14 \pm 0.20) \times 10^6 \text{ M}^{-2} \text{ s}^{-1}$ .

$$-d[\text{TPPMS}^-]/dt = k_{13}[\text{TPPMS}^-][\text{NO}]^2 \quad (14)$$

**TPPMS<sup>-</sup> as Analytical Reagent for NO.** The large rate constant and substantial associated absorbance changes in the UV, see Table 1, are attractive features for an analytical method for quantitative determination of small concentrations of NO. This idea was tested by using TPPMS<sup>-</sup> to quantify NO generated in the TMPD/HNO<sub>2</sub> reaction.

On the basis of the observed 1:1 TMPD/HNO<sub>2</sub> stoichiometry, and the value of the rate constant for the disappearance of TMPD approaching  $k_d$ , we concluded that only one of the nitrogen oxides generated in eq 1 reacted with TMPD. If both NO<sub>2</sub> and NO were reactive, then both the stoichiometry and the kinetics would be twice larger than observed. Moreover, TMPD does not have the potential to reduce NO, so that one should expect NO to accumulate in TMPD-HNO<sub>2</sub> solutions.

The reaction between TMPD (1 × 10<sup>-4</sup> M) and HNO<sub>2</sub> (5 × 10<sup>-5</sup> M) in 5.0 mM HClO<sub>4</sub> at 0.10 M ionic strength was allowed to go to completion (9600 s), as established by monitoring the absorbance increase at the 610-nm maximum of TMPD<sup>+</sup>. At that point, TPPMS<sup>-</sup> was injected (final concentration 7.86 × 10<sup>-5</sup> M) and the reaction with NO was monitored at 259 nm. From the absorbance decrease, we obtained [NO] = 3.81 × 10<sup>-5</sup> M, and from the initial rate we calculated  $k = 5.33 \times 10^6 \text{ M}^{-2} \text{ s}^{-1}$ . The excellent agreement between the measured rate constant and that determined independently for the TPPMS<sup>-</sup>/NO reaction confirms that the species reacting with TPPMS<sup>-</sup> was indeed NO. The concentration of NO was 76% of that calculated (5 × 10<sup>-5</sup> M) from the 1:1 TMPD/HNO<sub>2</sub> stoichiometry. We consider the agreement

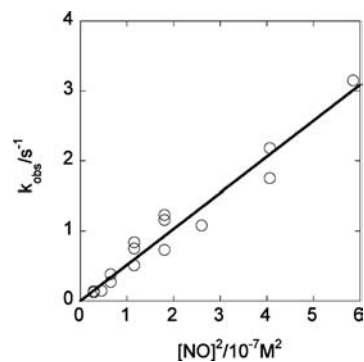


**Figure 5.** Plot of  $k_{\text{obs}}$  versus [NO]<sup>2</sup> for the reaction with TPPMS<sup>-</sup> in 2.0 mM HClO<sub>4</sub>. [TPPMS<sup>-</sup>] = 5 × 10<sup>-6</sup> M.

satisfactory in view of the slowness of the step that generated the NO. Despite all the precautions, some loss of NO to traces of air over such long times is unavoidable.

## Discussion

The NO/TPPMS<sup>-</sup> reaction in water closely parallels the NO/PPh<sub>3</sub> reaction in organic solvents.<sup>22</sup> In both cases the overall stoichiometry is [NO]/[Phosphine] = 2, kinetics are second order in NO, and N<sub>2</sub>O is produced, as in eq 13,14. The rates are, however, quite different; the oxidation of TPPMS<sup>-</sup> in H<sub>2</sub>O is orders of magnitude faster than the NO/PPh<sub>3</sub> reaction in toluene and chloromethanes, Table 2. Even though electron-donating substituents in the *para*-position have an accelerating effect on the PPh<sub>3</sub> reaction ( $\rho = -1.5$ , recalculated from data in ref 22 which reported  $\rho = -4.5$ ), even the most reactive phosphine studied, P(4-OCH<sub>3</sub>-C<sub>6</sub>H<sub>4</sub>)<sub>3</sub>, has a rate constant of only  $1.6 \times 10^3 \text{ M}^{-2} \text{ s}^{-1}$  in toluene.

The much greater reactivity of TPPMS<sup>-</sup> appears to be mostly solvent effect and not the electronic effect of a single sulfonate group on one of the phenyls. We base this conclusion on the magnitude of the effect, which is disproportionately large when compared to that observed in P(4-X-C<sub>6</sub>H<sub>4</sub>)<sub>3</sub>, see above. In those cases, the replacement of the most electron donating substituent (X = OCH<sub>3</sub>) with the most electron-withdrawing one (Cl) in all three phenyls caused the rate constant in toluene to decrease 260-fold. Upon introducing a sulfonate in a single phenyl in PPh<sub>3</sub> and changing the solvent to water, the rate constant increased 5.6 × 10<sup>4</sup>-fold. Even though the sulfonate renders the phosphine anionic, the electron density at phosphorus does not appear to be dramatically greater than in PPh<sub>3</sub>, as shown by the similarity of acidity constants for the protonated forms of PPh<sub>3</sub> (ca. 1 M, estimated from the data in H<sub>2</sub>O/CH<sub>3</sub>CN)<sup>38</sup> and TPPMS<sup>-</sup> (0.49 M, see above). The difference between the acidity constants for (4-X-C<sub>6</sub>H<sub>4</sub>)<sub>3</sub>P (X = Cl, H) are much greater, at least in the mixed H<sub>2</sub>O/CH<sub>3</sub>CN solvent.<sup>38</sup>

The strong solvent effect as well as the electronic effects in phenyl-substituted phosphines are both consistent with the two mechanisms already considered in the literature,<sup>22</sup> i.e., the reaction of the phosphine with NO dimer, eq 15, or the formation of a phosphine/NO adduct followed by the reaction with another molecule of NO, eq 16. This step generates

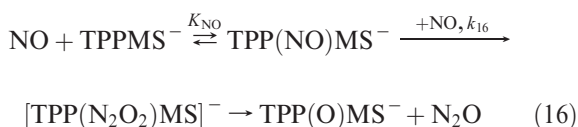
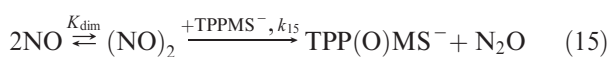
(38) Pestovsky, O.; Shuff, A.; Bakac, A. *Organometallics* 2006, 25, 2894–2898.

Table 2. Summary of Kinetic Data Obtained in This Work<sup>a</sup>

reaction	rate law <sup>b</sup>	stoich.	conditions	products
TPPMS <sup>-c</sup> + NO	$k[\text{TPPMS}^-][\text{NO}]^2$ $k = (5.14 \pm 0.20) \times 10^6 \text{ M}^{-2} \text{ s}^{-1}$	1:2	2–5 mM H <sup>+</sup>	TPP(O)MS <sup>-</sup> + N <sub>2</sub> O
PPh <sub>3</sub> + NO <sup>d</sup>	$k[\text{PPh}_3][\text{NO}]^2$ $k = (1.57 \pm 0.02) \times 10^3 \text{ M}^{-2} \text{ s}^{-1}$	1:2	CH <sub>2</sub> Cl <sub>2</sub>	OPPh <sub>3</sub> + N <sub>2</sub> O
PPh <sub>3</sub> + NO <sup>d</sup>	$k[\text{PPh}_3][\text{NO}]^2$ $k = (1.05 \pm 0.01) \times 10^3 \text{ M}^{-2} \text{ s}^{-1}$	1:2	CHCl <sub>3</sub>	OPPh <sub>3</sub> + N <sub>2</sub> O
PPh <sub>3</sub> + NO <sup>d</sup>	$k[\text{PPh}_3][\text{NO}]^2$ $k = 91 \pm 1 \text{ M}^{-2} \text{ s}^{-1}$	1:2	PhCH <sub>3</sub>	OPPh <sub>3</sub> + N <sub>2</sub> O
TMPD + HNO <sub>2</sub>	$k_d[\text{HNO}_2]^2$ <sup>e</sup>	1:1	2–5 mM H <sup>+</sup>	TMPD <sup>++</sup> + NO
ABTS <sup>2-</sup> + HNO <sub>2</sub>	$k_d[\text{HNO}_2]^2$ <sup>e</sup>	1:1	2–10 mM H <sup>+</sup>	ABTS <sup>•-</sup> + NO
ABTS <sup>2-</sup> + HNO <sub>2</sub>	$k_A[\text{ABTS}]_{\text{tot}}[\text{HNO}_2][\text{H}^+]$ $k_A = 695 \pm 16 \text{ M}^{-2} \text{ s}^{-1}$	1:1	0.2–0.8 M H <sup>+</sup>	ABTS <sup>•-</sup> + NO
TPPMS <sup>-</sup> + HNO <sub>2</sub>	$k_5 = (2.32 \pm 0.05) \times 10^9 \text{ M}^{-1} \text{ s}^{-1}$ <sup>f</sup> $4k_d[\text{HNO}_2]^2$ <sup>e</sup>	2:1	2–5 mM	TPP(O)MS <sup>-</sup> + NH <sub>2</sub> OH

<sup>a</sup> In acidic (HClO<sub>4</sub>) aqueous solutions at 298 K, unless stated otherwise. <sup>b</sup> For disappearance/formation of absorbing species (TPPMS<sup>-</sup>, PPh<sub>3</sub>, ABTS<sup>•-</sup>, TMPD<sup>++</sup>). The rate of disappearance of coreactants is related to the given rate law by the stoichiometric factor given in third column. <sup>c</sup> TPPMS<sup>-</sup> = P(C<sub>6</sub>H<sub>5</sub>)<sub>2</sub>(3-SO<sub>3</sub>-C<sub>6</sub>H<sub>4</sub>)<sup>-</sup>. <sup>d</sup> 294 K, see ref 22. <sup>e</sup>  $k_d = (10.9 + 175 [\text{H}^+]) \text{ M}^{-1} \text{ s}^{-1}$ , ref 13, see eq 1. <sup>f</sup> For reaction of NO<sup>+</sup> with ABTS<sup>2-</sup>/HABTS<sup>-</sup>.

TPP(N<sub>2</sub>O<sub>2</sub>)MS<sup>-</sup> intermediate, which eliminates N<sub>2</sub>O and forms TPP(O)MS<sup>-</sup>.



The preference for the second mechanism was expressed<sup>22</sup> on the basis of the small estimated equilibrium constant for the formation of (NO)<sub>2</sub> from NO in the gas phase ( $K_{\text{dim}} < 3 \times 10^{-4} \text{ M}^{-1}$ ),<sup>39</sup> and the assumption that  $K_{\text{dim}}$  has a similar value in toluene. In the meantime, the binding energy for (NO)<sub>2</sub> in the gas phase has been reported as only 696 cm<sup>-1</sup>,<sup>40</sup> again suggesting that the equilibrium concentration of N<sub>2</sub>O<sub>2</sub> in NO is extremely small and would require an exceptionally large rate constant,  $\sim 1 \times 10^5 \text{ M}^{-1} \text{ s}^{-1}$ , for the (NO)<sub>2</sub>/PPh<sub>3</sub> reaction to explain the experimental data. On this basis, the (NO)<sub>2</sub> route would seem to be disfavored.

The much greater rate constant for the NO/TPPMS<sup>-</sup> reaction observed in this work would seem to strengthen the antidimer case even more, provided that  $K_{\text{dim}}$  does not increase greatly in water. If this is the case, then the rate constant for the (NO)<sub>2</sub>/TPPMS<sup>-</sup> reaction would have to be unreasonably high, about  $1 \times 10^{10} \text{ M}^{-1} \text{ s}^{-1}$ , which would rule out the (NO)<sub>2</sub> route. Unfortunately, the value of  $K_{\text{dim}}$  is probably not constant across various solvents, and may well be much greater in water, leaving the (NO)<sub>2</sub> mechanism a (weak) possibility.

We prefer the mechanism in eq 16, not only by disfavoring eq 15, but also because the highly polar intermediate, [TPP<sup>δ+</sup>(NO)<sub>2</sub><sup>δ-</sup>MS]<sup>-</sup>, would be stabilized by polar solvents, thus explaining the strong positive effect of solvent polarity on the rate.

The rate constant for the NO/TPPMS<sup>-</sup> reaction was determined in this work in 2–5 mM HClO<sub>4</sub>, but the value obtained should remain unchanged at higher pH, including

pH 7, because neither reactant exhibits any acid/base chemistry in this pH range.

Regardless of the details, the fast NO/TPPMS<sup>-</sup> reaction in aqueous solutions does provide a convenient method for the determination of NO, as demonstrated in the HNO<sub>2</sub>/TMPD reaction which generates 1 equiv. of NO.

In its reactions with TMPD and ABTS<sup>2-</sup>, HNO<sub>2</sub> utilizes both mechanisms outlined in the Introduction. As expected, the mechanism in eqs 1–3 is prevalent at high [HNO<sub>2</sub>] and low [H<sup>+</sup>], i.e., conditions that favor second-order kinetics, whereas high [H<sup>+</sup>] activates the mechanism in eqs 4–6.

Both ABTS<sup>2-</sup> and TMPD are known to be oxidized by NO<sub>2</sub> with rate constants  $2.2 \times 10^7 \text{ M}^{-1} \text{ s}^{-1}$  (pH 7)<sup>41</sup> and  $1.8 \times 10^8 \text{ M}^{-1} \text{ s}^{-1}$  (pH 5.5, 40% CH<sub>3</sub>CN/H<sub>2</sub>O),<sup>33</sup> respectively. This fast one-electron oxidation draws the disproportionation equilibrium of eq 1 to the right and generates the observed products. As one would expect, the NO that is also generated in eq 1 does not react with either TMPD or ABTS<sup>2-</sup>, as shown by the overall 1:1 stoichiometry for the reaction of each with HNO<sub>2</sub>, and by finding close to one equivalent of NO in solution after completion of the TMPD/HNO<sub>2</sub> reaction.

The oxidation by NO<sup>+</sup> of both ABTS<sup>2-</sup> and TMPD is extremely rapid. The rate constant for ABTS<sup>2-</sup>/HABTS<sup>-</sup> obtained here is  $2.32 \times 10^9 \text{ M}^{-1} \text{ s}^{-1}$ , and that for TMPD is expected to also be close to diffusion controlled, given that TMPD is a much better reductant than ABTS<sup>2-</sup>. These rapid reactions with NO<sup>+</sup> make the mechanism in eqs 4–6 functional under the conditions that promote the formation of NO<sup>+</sup>, i.e., at high [H<sup>+</sup>].

**Oxidation of TPPMS<sup>-</sup> with HNO<sub>2</sub>.** In view of the second-order dependence on HNO<sub>2</sub>, some variant of the mechanism in eqs 1–3 must be operative. In a temptingly simple scenario, the disproportionation of HNO<sub>2</sub> would be followed by the reactions of TPPMS<sup>-</sup> with the nitrogen oxides formed. One might expect NO<sub>2</sub> to react by oxygen atom transfer, and NO as in eq 13. This mechanism, summarized in Scheme 1, predicts a 1:1 stoichiometry and N<sub>2</sub>O as product, clearly contradicting experimental facts, i.e., 2:1 stoichiometry and formation of NH<sub>2</sub>OH with a rate constant approaching  $4k_d$ .

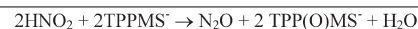
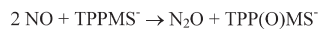
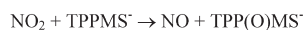
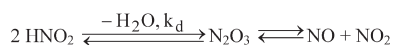
Undoubtedly, the second-order self-reaction of HNO<sub>2</sub> is still involved, but subsequent chemistry deviates from

(39) Forte, E.; Van den Bergh, H. *Chem. Phys.* **1978**, *30*, 325–331.

(40) Wade, E. A.; Cline, J. I.; Lorenz, K. T.; Hayden, C.; Chandler, D. W. *J. Chem. Phys.* **2002**, *116*, 4755–4757.

(41) Forni, L. G.; Mora-Arellano, V. O.; Packer, J. E.; Willson, R. L. *J. Chem. Soc., Perkin Trans 2* **1986**, 1–6.

## Scheme 1

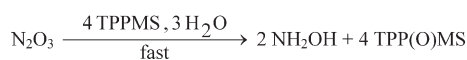
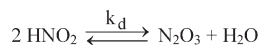


the simple picture in Scheme 1. The reaction of the phosphine with NO is known, and that with NO<sub>2</sub> might be reasonably assumed to involve intermediates. In the NO reaction, the evidence comes from the kinetics. Regardless of the exact nature of the intermediate, either (NO)<sub>2</sub> or phosphine-NO adduct, the reaction would be impeded at low, steady-state concentrations of NO, i.e., when the sole source of NO is eq 1. Under such conditions, the NO-phosphine reaction may take a different course than that shown in eq 13. In particular, the intermediate may react with additional phosphine when the supply of NO is extremely low. A similar situation would apply to the NO<sub>2</sub>-phosphine adduct.

It is also feasible, and perhaps more likely, that N<sub>2</sub>O<sub>3</sub>, formed in the first step in Scheme 1, reacts with the phosphine directly, without prior dissociation to NO and NO<sub>2</sub>. Several fast subsequent steps would follow to generate the observed products, Scheme 2. As pointed out by a reviewer, the first two-electron step in N<sub>2</sub>O<sub>3</sub>/TPPMS<sup>−</sup> reaction may generate HNO followed by the reaction of HNO with additional TPPMS<sup>−</sup> to yield NH<sub>2</sub>OH, similar to the reaction of HNO with thiolates.<sup>42</sup>

To some extent, our results also bear similarity to metal-mediated enzymatic<sup>43</sup> and electrocatalytic<sup>44</sup>

## Scheme 2



reduction of nitrite, where successive addition of electrons and protons to coordinated nitrogen species generates ammonia, hydroxylamine, and N<sub>2</sub>O. In contrast to those reactions, which are believed to be initiated by coordination of nitrite to the metal followed by coupled proton–electron transfers, the initial interaction with the phosphine does not involve HNO<sub>2</sub>/NO<sub>2</sub><sup>−</sup> but a product(s) of its bimolecular self-reaction, as established by the second order rate law of eq 12.

## Conclusions

In the reactions with TMPD and ABTS<sup>2−</sup>, HNO<sub>2</sub> utilizes two mechanisms, disproportionation and NO<sup>+</sup>-mediated oxidation, either one of which can dominate depending on the conditions. The disproportionation route generates NO and NO<sub>2</sub> followed by the fast NO<sub>2</sub>/substrate reaction. Nitrogen monoxide does not react with either of these substrates, but instead accumulates in solution, as confirmed with TPPMS<sup>−</sup> which we found to be a good analytical reagent for quantitative determination of NO in aqueous solutions. The reaction of nitrous acid with TPPMS<sup>−</sup> also involves bimolecular self-reaction of HNO<sub>2</sub>, but produces NH<sub>2</sub>OH, suggesting rapid follow-up steps between the phosphine and N<sub>2</sub>O<sub>3</sub>. No evidence was found for direct OAT from NO<sub>2</sub>.

**Acknowledgment.** We are grateful to the reviewers for useful and constructive comments. This work was supported by a grant from National Science Foundation, CHE 0602183. Some of the work was conducted with the use of facilities at the Ames Laboratory.

(42) Wong, P. S.-Y.; Hyun, J.; Fukuto, J. M.; Shirota, F. N.; DeMaster, E. G.; Shoeman, D. W.; Nagasawa, H. T. *Biochemistry* **1998**, *37*, 5362–5371.

(43) Einsle, O.; Messerschmidt, A.; Huber, R.; Kroneck, P. M. H.; Neese, F. *J. Am. Chem. Soc.* **2002**, *124*, 11737–11745.

(44) Barley, M. H.; Takeuchi, K. J.; Meyer, T. J. *J. Am. Chem. Soc.* **1986**, *108*, 5876–5885.